Eur. Phys. J. D **25**, 25–29 (2003)
DOI: 10.1140/epjd/e2003-00081-1

THE EUROPEAN PHYSICAL JOURNAL D

Towards controllable optical response of GaN quantum dots in alumina

C. Maurizio[1,a], G. Mattei[1], M.A. Garcia[1], E. Borsella[1,b], P. Mazzoldi[1], A. Quaranta[2], and F. D'Acapito[3]

[1] INFM, Dipartimento di Fisica, Università di Padova, Via Marzolo 8, 35131 Padova, Italy
[2] INFM, Dipartimento di Ingegneria dei Materiali, Università di Trento, Via Mesiano 77, 38050 Povo, Trento, Italy
[3] INFM, GILDA-CRG ESRF, B.P. 220, 38043 Grenoble, France

Received 23 October 2002 / Received in final form 20 February 2003
Published online 24 April 2003 –

Abstract. GaN nanocrystals (in the wurtzite phase) have been synthesized by thermal annealing in reducing atmosphere of Ga^++N^+ sequentially implanted alumina. We show that the reduction of Ga local concentration (by lowering the implantation dose) yields to an overall increase in the intensity of the GaN photoluminescence signal, to a decrease of the PL bandwidth and to the shift of its onset towards higher energies, due to quantum confinement effects in GaN nanocrystals with a narrow size distribution. The interpretation of the optical results is supported by structural analyses. Moreover, by investigating different forming treatments for GaN synthesis, the key role of hydrogen in the annealing atmosphere is evidenced.

PACS. 61.46.+w Nanoscale materials: clusters, nanoparticles, nanotubes, and nanocrystals – 81.05.Ea III-V semiconductors – 78.67.Hc Quantum dots – 85.40.Ry Impurity doping, diffusion and ion implantation technology

1 Introduction

Among the semiconductor binary nanostructures [1], those formed by gallium nitride are most studied, especially in recent years, for their technological application in the realization of blue-green light emitting diodes and laser, high-speed field-effect transistors, UV photodetectors and high-power devices, owing to the wide optical bandgap of wurtzite GaN (E_g = 3.45 eV). Moreover, GaN is a promising candidate for high-temperature electronic devices due to its strong atomic bonding. Not only the synthesis of quantum dots, but also of heterostructures such as GaN nanowires, tubes [2], thin films [3] and quantum wells attracts much interest. The importance of nanometer-sized gallium nitride crystals is based on their photoluminescence properties: they exhibit quantum-confinement effects that allow tailoring the optical properties of the system. Several different techniques have been explored and used for the fabrication of GaN nanocrystals; most of the methods are based on colloidal chemistry [4], reactive laser ablation [5,6], epitaxy [7] and chemical vapor deposition [8]; anyway, the difficulty in developing synthesis methods for the growth of high-quality GaN nanocrystals, especially for their photoluminescence response, is not solved yet [9]. About the synthesis of GaN nanocrystals in dielectric matrices, sequential ion implantation [10] of Ga^++N^+ ions was demonstrated to be a very promising technique if followed by proper thermal annealing in NH_3 atmosphere (at T = 900 °C for 1 h) [11,12]. Furthermore, it was established that the role of N^+ implantation after the Ga^+ one is both to prevent Ga outdiffusion and to initiate GaN synthesis, by inducing the formation of Ga oxynitrides into the matrix [11]. In addition, the aggregation of crystalline clusters can be promoted in amorphous or amorphized networks, so ruling out the mandatory need of a template to induce the coherent growth of the precipitates [11]. Nevertheless, there are still some open questions on the role and nature of the processes that drive GaN clusters formation; as for the post-implantation annealing treatments for GaN synthesis, it is not yet clear whether the use of nitrogen-supplying atmosphere is mandatory for crystalline nitride formation, or implanted nitrogen atoms can directly aggregate in nanocrystals during thermal annealing in reducing atmosphere. Detailed investigations are fundamental to fabricate systems with a narrow and intense photoluminescence band, whose range energy could be tuned by quantum confinement effects. In this article, we report on the morphological and optical characterization of systems prepared by sequential ion implantation of Ga and N ions into α-alumina. The main purpose is to investigate the role of implantation doses and different reducing annealing atmospheres in determining the composite structure, with the aim at improving the optical response of these systems.

[a] *Present address:* INFM, GILDA-CRG ESRF, B.P. 220, 38043 Grenoble, France. e-mail: `maurizio@padova.infm.it`
[b] *Permanent address:* ENEA-UTS FIS, Via E. Fermi 45, 00044 Frascati (Rome), Italy.

Table 1. Ion implantation and heat-treatment parameters for the prepared samples; all the annealing treatments were performed at $T = 900$ °C for 1 h.

sample name	Ga^+ implant dose (Ga^+/cm^2), energy (keV)	N^+ implant dose (N^+/cm^2), energy (keV)	annealing atmosphere
A5	10×10^{16}, 120	12×10^{16}, 30	NH_3
A6	6×10^{16}, 120	4×10^{16}, 30	NH_3
A7	3×10^{16}, 190	4×10^{16}, 40	NH_3
	1.1×10^{16}, 100	-	NH_3
A8	3×10^{16}, 190	4×10^{16}, 40	H_2(4%)/Ar
	1.1×10^{16}, 100	-	

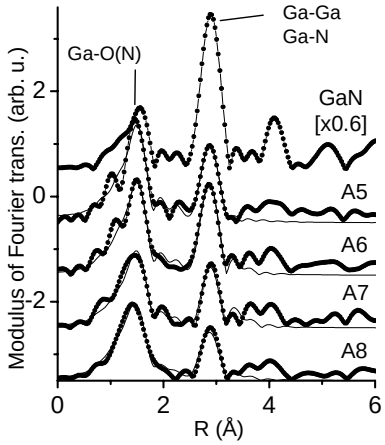

Fig. 1. k^2-weighted Fourier transform moduli (in the range $k = 2.6{-}13.0$ Å^{-1}) of EXAFS spectra (solid line with markers) recorded at Ga K-edge from the samples obtained by Ga+N implantation in alumina at different doses (see Tab. 1), after annealing in NH_3 (samples A5, A6, A7) or in H_2 (sample A8); the peaks of Ga–O/Ga–N and Ga–Ga coordinations are indicated, and the corresponding fits are also shown (solid line without markers); the spectrum from wurtzite GaN is reported for comparison.

2 Experimental

The parameters for the Ga^++N^+ sequential ion implantation, performed at room temperature, are reported in Table 1; for the samples A7 and A8 two Ga^+ implantations at different energies were performed to obtain a region (about 50 nm thick) with a homogeneous Ga concentration. The Ga and N concentration depth profiles were preliminary evaluated by means of the SRIM2000 code, that calculates the stopping range of ions into matter using a quantum mechanical treatment of the ion-atom collisions [13]: the maximum of the dopant concentration was estimated at about 90 nm from the surface for the A5 and A6 samples, and from 80 to 120 nm for the A7 and A8 samples (double Ga implantation). After ion implantation, the samples were heated in ammonia or hydrogen (4%) atmosphere for 1 hour at $T = 900$ °C. Gallium concentration profiles and actual fluences were measured by Rutherford backscattering spectrometry (RBS): a good agreement between the calculated and measured Ga projected ranges was detected. Transmission electron microscopy (TEM) and selected area electron diffraction (SAED) analyses were performed with a Philips CM30T, operating at 300 kV, on cross-sectional samples thinned with an Ar^+-ion milling system at liquid nitrogen temperature. Extended X-ray absorption fine structure (EXAFS) spectroscopy and grazing incidence X-ray diffraction (GIXRD) analysis were performed at the European Synchrotron Radiation Facility (Grenoble, France), on the Italian beam-line GILDA (details on the experiment and data analysis in Ref. [11]) and on ID09 beam-line (details in Ref. [14]), respectively. Photoluminescence (PL) spectra of the implanted samples were recorded over the temperature range 77−300 K. The frequency doubled emission of a N_2-laser pumped dye-laser (500 ps pulse duration) was used as exciting source. The emission spectra were dispersed by an ORIEL MS257 monochromator (focal length 0.25 m) equipped with a fast photomultiplier. The time resolved PL signals were acquired by a TDS 7104 TEKTRONIX Transient Digitizer with maximum digital storage sampling rate of 10 Gsamples/s and 1 GHz bandwidth.

3 Results and discussion

To investigate the effect of the implantation doses on the composite structure after the NH_3-annealing, the Ga K-edge EXAFS spectra for the samples A5 (high-dose implantation) and A6 (low-dose), recorded in the fluorescence mode at 77 K were analyzed.

In Figure 1 the Fourier transforms of the EXAFS spectra of the implanted samples are compared to the spectrum recorded in transmission mode at 77 K on a sample of crystalline GaN (wurtzite) grown by molecular beam epitaxy. The main features of GaN spectrum are well reproduced for all the samples. For quantitative analysis of the spectra from the samples, the S_0^2 value [15] was estimated from the analysis of the GaN bulk spectrum. The fit in R-space of the first two coordination shells used the phases and amplitudes calculated with the FEFF8 code for the structure of crystalline GaN [16]. Fitting results are reported in Table 2 and fit quality is shown in Figure 1: the comparison with the parameters that characterize the Ga local structure in GaN bulk indicates that the structures typical of GaN phase are formed in both samples. Furthermore, part of Ga atoms (not more than about 50%) remain dispersed in the matrix, bonded with light atoms (O and/or N, EXAFS not being able to distinguish between the two backscatterers); this emerges from the comparison between the first two shells because the second one (Ga–Ga and Ga–N coordinations) takes contribution only from GaN clusters, while the first one (Ga–O and Ga–N coordinations) accounts for both Ga atoms dispersed in the matrix and for Ga atoms aggregated in GaN clusters. The fitting results are very similar for the two samples, indicating that the average local structure around Ga atoms does not depend on the implantation fluences in the two examined conditions. On the other

Table 2. Fitting results (first two coordination shells) of Ga K-edge EXAFS spectra for the alumina samples implanted with Ga+N ions at different doses (see Tab. 1), after annealing in NH_3 (samples A5, A6, A7) or in H_2(4%) (sample A8), compared to those obtained from the EXAFS spectrum of bulk GaN (in parenthesis); the crystallographic data of wurtzite GaN are reported for comparison.

sample		A5	A6	A7	A8	GaN bulk
	N	3.9 ± 0.5	4.0 ± 0.6	3.4 ± 0.7	3.9 ± 0.8	3, 1
I shell	R (Å)	1.93 ± 0.02	1.94 ± 0.02	1.94 ± 0.02	1.93 ± 0.02	1.9493, 1.9562
Ga–N						(1.97 ± 0.02)
	σ^2 (10^{-4} Å^2)	28 ± 16	36 ± 17	37 ± 25	55 ± 28	(65 ± 26)
	N	5.1 ± 1.8	5.8 ± 1.1	2.0 ± 1.1	3.0 ± 1.3	6, 6
II shell	R (Å)	3.19 ± 0.02	3.20 ± 0.02	3.22 ± 0.02	3.20 ± 0.02	3.1816, 3.1900
Ga–Ga						(3.21 ± 0.02)
	σ^2 (10^{-4} Å^2)	60 ± 23	59 ± 12	16 ± 32	52 ± 29	(24 ± 7)
	N	3.8 ± 1.3	4.3 ± 0.8	4.7 ± 2.4	2.2 ± 0.9	9
II shell	R (Å)	3.75 ± 0.02	3.76 ± 0.02	3.78 ± 0.02	3.77 ± 0.02	3.7383
Ga–N						(3.78 ± 0.02)
	σ^2 (10^{-4} Å^2)	116 ± 272	14 ± 76	14 ± 9	13 ± 160	(68 ± 108)

hand, TEM and SAED analyses show the presence of GaN nanocrystals (in wurtzite phase) only for the A5 sample (high-dose implantation) [11], while no clusters could be observed for the low-dose implanted sample. Actually, the GaN clusters possibly present have a faint contrast with respect to the matrix [11]; in addition, even if the matrix is completely amorphized in the implanted region [11], it is known that the subsequent NH_3 annealing process determines a partial recrystallization of the matrix according to the γ crystalline phase [17]. Thus, the contribution of both Al_2O_3 crystalline substrate (present below the implantation range) and of the γ crystalline phase (in the implanted region) in SAED pattern could hide the diffraction signal from the small GaN clusters possibly present. The results obtained indicate that large GaN clusters are present only in the A5 sample (high-dose implantation), while the size of the GaN clusters evidenced by EXAFS spectroscopy in the sample A6 (low-dose), is below the detectable limit for TEM in this particular sample. As the size of the GaN nanocrystals is comparable to the excitonic Bohr radius ($a_0 \simeq 3$ nm for GaN [18]), quantum confinement effects are expected to arise. The variation of the energy gap of GaN nanocrystals as a function of their size, calculated according to reference [19], is reported in Figure 2a. The PL spectra taken on all the samples upon excitation at 4.24 eV are shown in Figure 2b. In agreement with the quantum confinement theory, the onset of the PL emission for the A5 (high-dose) and A6 (low-dose) samples appears to be shifted towards higher energy as compared to bulk GaN in wurtzite phase (bandgap energy $E_g = 3.45$ eV). Moreover, the comparison between the two spectra highlights that the implantation dose dramatically affects the PL spectra. In the high-dose implanted sample A5, the presence of large clusters as well as the high concentration of defects lead to a broad spectrum; on the other hand, the emission spectrum of sample A6 (low-dose implanted sample) is narrower and shifted towards higher energy, suggesting a narrower cluster size distribution of small clusters (according to the structural analyses discussed).

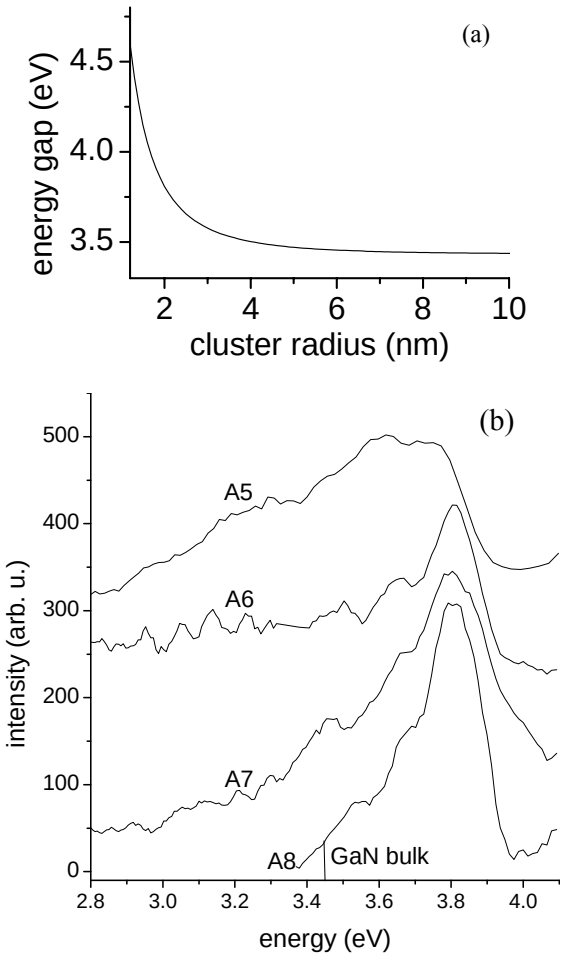

Fig. 2. (a) Energy gap of GaN nanocrystals as a function of cluster radius, calculated according to reference [19]. (b) PL spectra taken on the samples obtained by Ga+N implantation in alumina at different doses (see Tab. 1), after annealing in NH_3 (samples A5, A6, A7) or in H_2 (sample A8), at an excitation energy of 4.24 eV ($T = 110$ K); the energy gap of GaN bulk is also indicated.

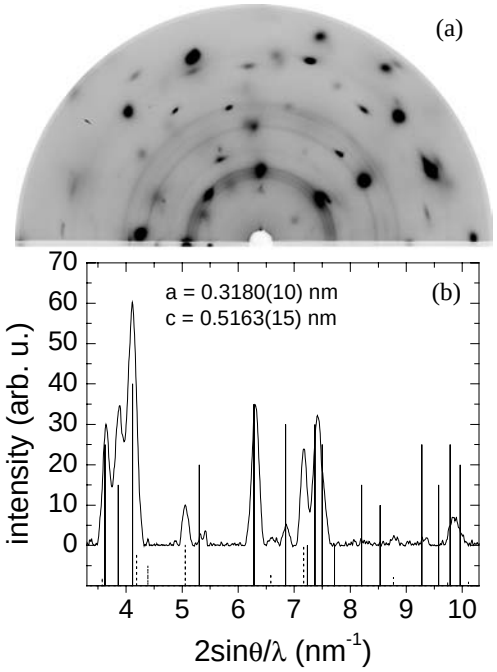

Fig. 3. (a) GIXRD pattern of Ga+N implanted alumina, after annealing in H_2(4%) (sample A8). Besides the strong reflections from the crystalline matrix, the Debye Scherrer rings from the nanocrystals are clearly visible. (b) Radially integrated scattering profile of the GIXRD pattern (the most intense peaks from the matrix were masked) after background subtraction. Vertical bars indicate the reflection positions from the crystalline wurtzite GaN (solid lines) and from the γ-Al_2O_3 (dashed lines).

To investigate the role of thermal annealing in different atmospheres on the efficiency of GaN nanocrystal fabrication and on the relative photoluminescence properties, two more samples, prepared by low-dose Ga+N implantation, were processed by two different post-implantation thermal annealing in reducing atmosphere, either ammonia (A7 sample) or H_2(4%):Ar(96%) (A8 sample); for these samples the local concentration of dopants is lower than for the A6 sample (see Tab. 1). The EXAFS analysis (see Tab. 2 and Fig. 1) evidenced the formation of GaN structures, as well as the presence of Ga dispersed in the matrix. With respect to the A6 sample, the peak in the Fourier transform modulus, related to the second shell of atoms around Ga in the samples A7 and A8, is lower, indicating that the percentage of Ga atoms dispersed is higher than in the previous cases. This is confirmed by the Ga–Ga coordination number for the two samples, lower than that of samples A5 and A6 (see Tab. 2). For the analysis of the spectrum of the sample A7, the ratio between the Debye-Waller factors of the two Ga–N coordinations was fixed to the value for sample A6, and no constraints were imposed on the coordination numbers; anyway, this did not alter significantly the fitting results. The crystalline structure was investigated for the sample A8 by means of GIXRD: in the diffraction pattern reported in Figure 3a, besides the strong reflections from the crystalline matrix, the Debye-Scherrer rings of crystalline, randomly oriented GaN nanoparticles are clearly visible. After radial integration and background subtraction, the analysis of the diffraction signal from the nanocrystals (Fig. 3b) indicates that the measured lattice constants ($a = 0.3180(10)$ nm, $c = 0.5163(15)$ nm) agree well with those of bulk wurtzite GaN ($a = 0.3186$ nm, $c = 0.5178$ nm). The photoluminescence analyses on samples A7 and A8 show that the intensity of the PL band is enhanced with respect to the A5 and A6 samples and that its onset is shifted toward higher energies (see Fig. 2b). The EXAFS and PL findings suggest that the population of small GaN clusters is increased with respect to the A5 and A6 samples, because of the lower local Ga concentration in the implanted region. Moreover, some indication can be drawn on the effectiveness of annealing atmosphere for GaN clusters synthesis, and consequently on the photoluminescence properties of the obtained systems. As far as the annealing in H_2/Ar is concerned, the results from PL, GIXRD and EXAFS analyses on the sample A8 indicate that this heating treatment properly induces GaN cluster synthesis: hydrogen diffusing into the sample acts as a reducing agent for the Ga oxide-oxinitrides formed by double Ga^++N^+ implantation. This process is effective for a thermal treatment at 900 °C: the fact that the same annealing at higher temperature (1200 °C) did not result in GaN clusters [11] is likely ascribable to the onset, at high temperature, of the thermal decomposition of the GaN clusters possibly formed. The effectiveness of H_2(4%) annealing for GaN synthesis sheds some light also on the processes involved in GaN aggregation upon annealing in ammonia atmosphere (sample A7): since at 900 °C the dissociation of ammonia in N_2 and H_2 molecules is fairly complete [20], it can be claimed that also in this case the diffusion of hydrogen from the atmosphere into the sample is the main responsible of the GaN nanocluster formation. Thus, it turns out that, in alumina matrix doped with both Ga and N, the use of nitrogen-supplying atmosphere is not needed for crystalline gallium nitride formation. Moreover, even if the H_2 concentration at $T = 900$ °C is expected to be higher in totally or partially dissociated ammonia than in the H_2/Ar atmosphere, this did not determine strong differences between the PL spectra of the A7 (NH_3-annealed) and A8 (H_2-annealed) samples, thus indicating a saturation effect in the hydrogen reaction with Ga-oxides and oxynitrides at low Ga concentrations. Concerning the lifetime of the GaN nanocrystal excitons measured in our systems, the PL time decay curves at 77 K for the 325 nm emission showed an exponential decay with a time constant around 10 ns. Excitons lifetime for GaN at low temperature is usually given in literature between 0.1 and 1 ns [21–24]. Several reasons could account for the difference with the experimental results obtained here. It is well established that in nanocrystals, quantum confinement effects increase the binding energy of the excitons [7,25] and recently it was pointed out that for GaN, higher binding energy yields to an increase in the exciton lifetime [26]. Thus, a larger time constant is expected for nanocrystals than for bulk GaN. However, considering the size of the

nanocrystals as measured by TEM ($\simeq$2 nm), the binding energy of the excitons could increase of about 20 meV [25], yielding to an increase in the lifetime of about 0.5 ns, that can only account partially for the longer measured lifetime. GaN excitons lifetime is mainly determined by the non-radiative transitions which are favoured by the presence of impurities. In particular, a doping level below 10^{16} cm^{-3} increases the lifetime over 1 ns [27]. In the case of low impurity concentration, the lifetime increases with the temperature and reaches about 10 ns at $T = 100$ K. Hence, the larger exciton lifetime reported here suggests that the synthesized nanocrystals have a low degree of impurities. This is particularly important for the case of hydrogen impurities (involved in the synthesis process) as they are known to reduce PL intensity, limiting potential applications of the material [21].

4 Conclusions

In conclusion, we have shown that in the process of GaN synthesis upon annealing in NH_3 of Ga^++N^+ sequentially implanted alumina matrix, the use of low-dose Ga^++N^+ implantation (with respect to Ref. [11]) greatly improves the photoluminescence signal from the GaN clusters. The GaN photoluminescence band exhibits quantum confinement effects and results narrower than in the case of high-dose implantation, suggesting the presence of a narrower size distribution of smaller clusters, according to EXAFS and TEM results. Further reduction of the Ga local concentration increases the GaN photoluminescence signal and shifts the onset of the PL signal toward higher energies. Moreover, it was demonstrated that a thermal annealing in H_2(4%) at 900 °C for 1 h is effective for GaN clusters synthesis, by chemical reduction of the Ga oxide-oxinitrides formed after implantation: this strongly suggests that also during the annealing in ammonia at the same temperature the key role for GaN synthesis is played by the hydrogen molecules present in the atmosphere due to the almost complete NH_3 thermal decomposition.

The technical assistance of M. Parolin at INFN-INFM Ion Implantation Laboratory is gratefully acknowledged. This work has been partially supported by MURST National University Research Project and by Italian CNR National Project MST-II.

References

1. A.P. Alivisatos, Science **271**, 933 (1996)
2. M. He *et al.*, Appl. Phys. Lett. **77**, 3731 (2000)
3. B. Daudin *et al.*, Mat. Sci. Eng. B **50**, 8 (1997)
4. O.I. Micic, S.P. Ahrenkiel, D. Bertram, A. Nozik, Appl. Phys. Lett. **75**, 478 (1999)
5. T.J. Goodwin *et al.*, Appl. Phys. Lett. **70**, 3122 (1997)
6. V.J. Leppert *et al.*, Appl. Phys. Lett. **72**, 3035 (1998)
7. P. Ramvall *et al.*, Appl. Phys. Lett. **73**, 1104 (1998)
8. S. Tanaka *et al.*, Appl. Phys. Lett. **71**, 1299 (1997)
9. C.M. Balcas, R.F. Davis, J. Am. Ceram. Soc. **79**, 2309 (1996)
10. A. Meldrum, R.F.J. Haglund, L.A. Boatner, C.W. White, Adv. Mater. **13**, 1431 (2001)
11. E. Borsella *et al.*, J. Appl. Phys. **90**, 4467 (2001)
12. J.A. Wolk, K.M. Yu, E.D. Bourret-Chourchesne, E. Johnson, Appl. Phys. Lett. **70**, 2268 (1997)
13. J.P. Biersack, L.G. Haggmark, Nucl. Instr. Meth. **174**, 257 (1980)
14. F. D'Acapito, F. Zontone, J. Appl. Cryst. **32**, 234 (1999)
15. J.J. Rehr, R.C. Albers, Rev. Mod. Phys. **72**, 621 (2000)
16. A. Ankudinov, B. Ravel, J.J. Rehr, S.D. Conradson, Phys. Rev. B **56**, 7565 (1990)
17. J.D. Budai *et al.*, Nature **390**, 384 (1997)
18. W. Orton, C.T. Foxon, Rep. Prog. Phys. **61**, 1 (1998)
19. A.D. Yoffe, Adv. Phys. **42**, 1 (1993)
20. S.J. Pearton, J.C. Zolper, R.J. Shul, F. Ren, J. Appl. Phys. **86**, 1 (1999)
21. G.D. Chen *et al.*, Appl. Phys. Lett. **67**, 1653 (1995)
22. M. Smith *et al.*, Appl. Phys. Lett. **67**, 3387 (1995)
23. G.D. Chen *et al.*, J. Appl. Phys. **79**, 2675 (1996)
24. M. Smith *et al.*, J. Appl. Phys. **79**, 7001 (1996)
25. P. Ramvall *et al.*, J. Appl. Phys. **87**, 3883 (2000)
26. O. Brandt *et al.*, Phys. Rev. B **58**, R15977 (1998)
27. L. Eckey *et al.*, Appl. Phys. Lett. **68**, 415 (1996)